Sādhanā (2021)46:233
https://doi.org/10.1007/s12046-021-01760-8

An experimental study on mechanical properties and wear of A380/ nB_4C composites fabricated using two different liquid state processes

JAIVIR SINGH[1,*], NOE ALBA-BAENA[2], RAJEEV TREHAN[1] and VISHAL S SHARMA[3]

[1]Department of Industrial and Production Engineering, Dr B R Ambedkar National Institute of Technology, Jalandhar, Punjab, India
[2]Department of Industrial and Manufacturing Engineering, Institute of Engineering and Technology, Autonomous University of Ciudad Juarez, Chihuahua, Mexico
[3]School of Mechanical, Industrial and Aeronautical Engineering, University of the Witwatersrand, Johannesburg, South Africa
e-mail: jsjaivirsingh@gmail.com; nalba@uacj.mx; trehanr@nitj.ac.in; vishal.sharma@wits.ac.za

MS received 5 July 2021; revised 21 September 2021; accepted 5 October 2021

Abstract. In the present work, fabrication of metal matrix composite of aluminium alloy A380 reinforced with 0.5, 1 and 1.5 weight percentages of nano boron carbide through mechanical stirring and ultrasonic treatment processes. Scanning Electron Microscopy (SEM), Back Scattered Electron Detector (BSE) and energy-dispersive X-ray spectroscopy (EDS) are used to characterize fabricated composites. Furthermore, tensile, hardness and wear tests are performed to compare the mechanical and wear properties of prepared samples. It is found that UST is an efficient process as compared to MS for refining the microstructure of base alloy and fabricated composites. Also, the reinforced particles are efficiently and uniformly distributed in the ultrasonic treatment process. The improved properties of the ultimate tensile strength (UTS) and hardness observed at A380/1nB_4C as 57%, and 35% respectively and wear of the fabricated composites samples is less as compared to the base alloy.

Keywords. Nanocomposites; Aluminium A380; Boron Carbide; Ultrasonic Treatment; Mechanical Stirring; Wear.

1. Introduction

The demand for low cost, lightweight and quality products is increasing and aluminium and its alloys play a key role to meet the current scenario demands. Aluminium alloy A380, is widely used in the manufacturing and die casting industries due to its lightweight and remarkable properties of good fluidity, resistance to hot cracking and wear. Also, it is used in a variety of applications in the automotive industries for the manufacturing of brake casting, gear cases, cylinder head and engine blocks. To fulfil market demands, the materials must provide better mechanical properties, which are difficult for a monolithic material and alloy. To achieve improved mechanical and tribological properties, aluminium metal matrix composites (AMMC) are promising materials for automobile, aerospace, structural, military, and marine industries. AMMC provides high strength to weight ratio, high hardness, high compressive strength, low coefficient of thermal expansion, improved wear and corrosion resistance properties as compared to aluminium alloy. Further to enhanced properties, the ceramics particles are added as reinforcement in the aluminium metal matrix. The common reinforcements are alumina, SiC, TiC, Fly-ash, red mud, and rice husk. Furthermore, B_4C reinforcement is a promising ceramic for the aluminium metal matrix. This is because B_4C possesses a broad spectrum of applications due to its excellent material properties like high hardness, low specific gravity, chemically stable and high elastic modulus. Also, the mixing, distribution and particle size of reinforcement play an important role in metal matrix composite [1–5].

In order to achieve proper mixing conditions, many researchers used the stirring process. Garcia-Rodríguez *et al* [6] analysed the flow patterns to identify the better conditions for using mechanical stirring for the distribution of particles and to achieve homogeneous mixing. The parameters like mixing time, stirring speed (100 to 1200 rpm), impeller angle (0°, 15° and 30°), vortex height and its behaviour in different fluids play a vital role. The processing parameters are used to achieve higher mixing and distribution efficiency. In other studies, the proper mixing of the reinforcement in molten metal is achieved with the mechanical stirring process [7, 8]. Aurandi *et al* [9] used the stir casting two-step addition method for Al 6061 and 5,

*For correspondence
Published online: 30 October 2021

7 wt.% of B_4C particles with K_2TiF_6 to avoid agglomeration and improved wettability. LI *et al* [10] used modified vacuum mechanical stirring equipment for 31% mass fraction of B_4C as reinforcement in AA6061 aluminium matrix. This study demonstrated the uniform distribution of particles and less porosity occurred in vacuum casting as compared to casting at atmospheric pressure. In industrial conditions, processes are used under atmospheric pressure because in vacuum casting there is the size limitation of cast product and if large casting produces with vacuum casting the cost of the product will be high. Park *et al* [11] used stir casting and an automated quantification technique for dispersion of reinforcement in the aluminium matrix.

In order to achieve the proper mixing and enhanced mechanical properties, other processes are also used. Alba *et al* [12] used ultrasonic processing to study melt degassing and structure modification in aluminium alloys. Ultrasonic processing reduced the porosities and achieved the refined grain structure of alloys. Singh *et al* [13] prepared a hybrid nanocomposite of Al 7075 with alumina and graphite as reinforcement materials using stir and ultrasound-assisted casting methods. Miranda *et al* [14] studied mechanical properties of composite LM24 as matrix material and Cu-carbon nanotube as reinforced with ultrasonic cavitation process. They reported that the ultimate tensile strength and yield strength of composite improved with a decline in elongation. In other studies, the effect of the ultrasonication process is studied on composites of aluminium and its alloy with B_4C at different weight percentages. They reported that proper mixing and distribution of B_4C particles are achieved with the use of an ultrasonic process [15–17]. Sun *et al* [18] studied the microstructure and mechanical properties of pure aluminium and silicon carbide in the form of particulate of diameter (4.7, 16.7, 39.1 and 70.7 μm) composite using powder metallurgy process. They reported that with the reduction in the size of SiC particulate, tensile strength and yield strength of fabricated composite improved. The authors in other studies are also suggested a cavitation-based high-intensity ultrasonic process for the distribution of nanoparticles in metal melts to achieve promising results [19–21].

Many methods are used for the fabrication of AMMC such as mechanical alloying [22, 23], high energy ball milling [24], powder metallurgy, spray deposition and laser deposition, etc. The above solid-state methods are expensive, energy-consuming and have limitations of size and complexity in parts [25]. Mechanical stirring process is low cost, simple operation and no size limitation in parts fabrication mostly used as liquid state method. Further, the stir casting process uniformly distributes micro size particles

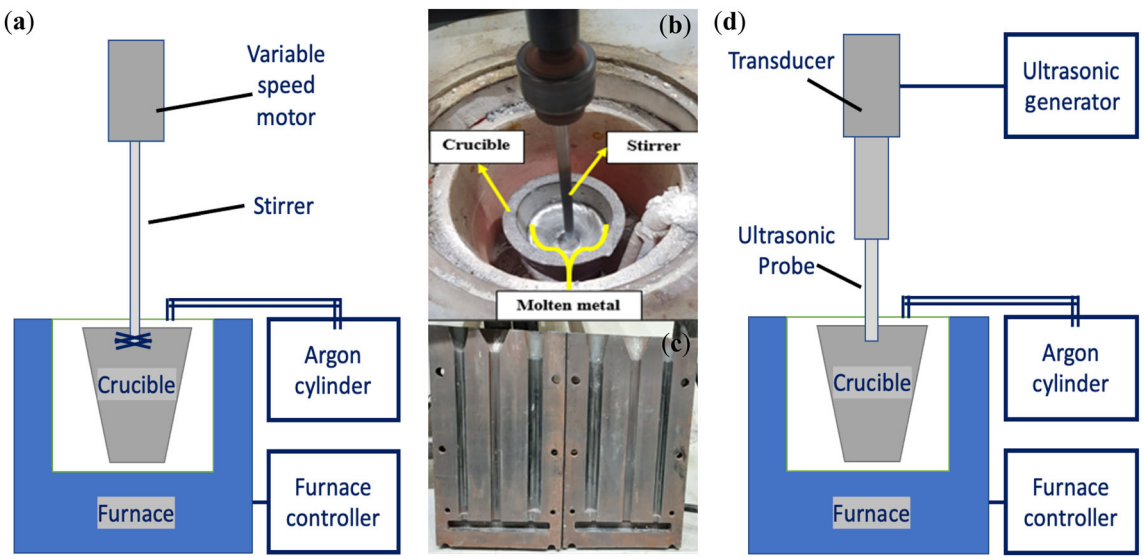

Figure 1. Experimental set-up used in this study: (a) Mechanical stirring set-up, (b) impeller position during MS processing, (c) Mold and (d) Ultrasonic treatment set-up.

Table 1. Chemical composition of initial A380 ingot.

Si	Cu	Fe	Mg	Mn	Ni	Zn	Pb	Sn	Ti	Others	Al
8.58	3.28	0.915	0.086	0.287	0.059	1.631	0.088	0.031	0.031	0.053	84.99

Table 2. Composition and characterization of nB_4C particles.

Name	Formula	colour	Form	Molecular weight (g/mol)	Melting point (°C)	Particles size (nm)	Purity (%)	B	C	Others
Boron carbide	B_4C	Black	Powder	55.251	2763	<100	99.9	77.98	21.92	0.1

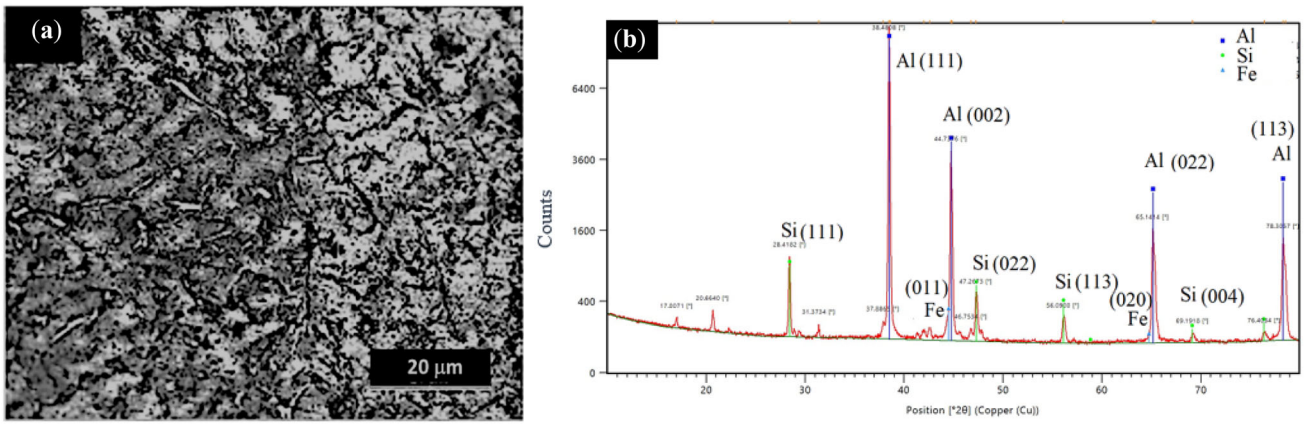

Figure 2. Images from the A380 ingot: (a) selected Optical Micrograph and (b) XRD profile.

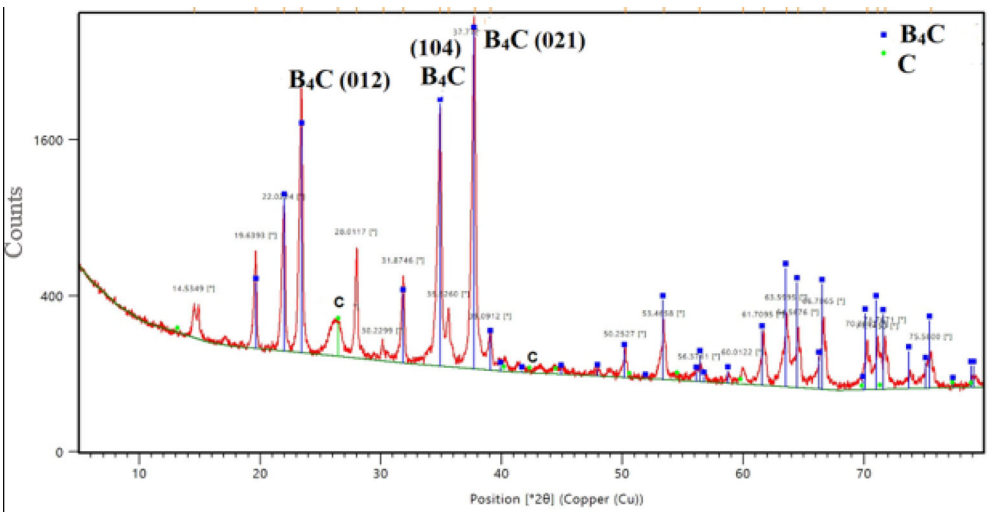

Figure 3. XRD profile of received nB_4C powder.

efficiently [16] and there is the formation of the cluster [26] with the reduction in reinforced particles size. After going through the literature it is observed that the quantity of reinforced material is high in matrix material due to which many issues like non-uniform particles distribution and particles agglomeration raised [27–29]. Using high quantity reinforcement, the manufacturing cost of the product is increased which includes the cost of reinforced particles and post-processing cost. Furthermore, to overcome these issues in the casted samples less quantity of reinforcement and ultrasonic treatment is the possible solution. The purpose of this work is to fabricate A380/nB_4C composites through mechanical stirring (MS) and ultrasonic treatment (UST) processes using less quantity of reinforcement.

Optical microscope (OM), Scanning electron microscopy (SEM), Back Scattered Electron Detector (BSE) and energy-dispersive X-ray spectroscopy (EDS) are used to characterize fabricated composites. Further, composite samples are tested for mechanical properties (tensile and hardness) and wear test at dry sliding condition.

2. Experimental procedure

Samples are cut from aluminium alloy A380 ingot (Century NF casting, India), as base data values for the fabrication of the different A380/nB_4C composites. Samples of boron carbide powder are used to characterize nanoB_4C (nB_4C) particles supplied by Nano Research Elements India. The X-ray profile is used from the X-ray diffractometer (XRD) (Malvern Panalytical, model: 3rd generation Empyrean) to analyse the initial composition of aluminium alloy A380 and B_4C composition. The optical image of aluminium alloy A380 is obtained using an optical microscope (OM) (Leica, model: DM2700M) and the particles size of B_4C powder is measured using a field emission scanning electron microscope (FESEM) (JEOL, model: JSM7610F).

Samples are prepared for fabrication of A380/nB_4C (0, 0.5, 1 and 1.5 wt.%) composites using the mechanical stirring (MS) set-up as shown in figure 1(a). The mechanical stirrer has a maximum rotation speed of 1000 rpm in both directions (clockwise and anticlockwise). It consists of a steel rod and 3 blades impeller of titanium material. The blades of the impeller are inclined at an angle of 30° with 5 mm thickness, 15 mm height and periphery of 40 mm. The impeller is dipped in molten metal up to the one-third position from the bottom at a rotation speed of 700 rpm shown in figure 1(b). The second process for ultrasonic treatment (UST), the ultrasonic setup of make Textsonic (India), using 20 kHz frequency, 5 kW power and a niobium probe of 250 mm in length and 20 mm in diameter.

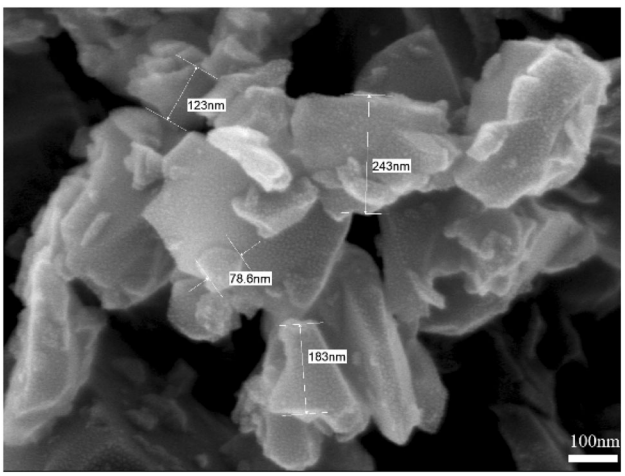

Figure 4. SEM Image from received B_4C powder.

The graphite crucible has an outer diameter of 105 mm, height 127 mm, bottom outer diameter 70 mm and capacity of 3.7 kg is used for experimentation. The electric muffle furnace of 3 kg capacity, 5 kW power, with a nichrome 80–20 heating element and 1.83 mm diameter, 10 mm coil diameter and maximum temperature up to 1000°C (Kanthal, UK). Figure 1(d) illustrates the experimental setup arrangement as used in the present study.

The matrix metal A380 is cut into small pieces and properly cleaned. The reinforcement particles nB_4C are preheated at 250°C for 2.5 h in a muffle furnace, the mold is preheated at 350°C and powder samples are prepared for 0% (as reference), 0.5, 1 and 1.5 wt.% nB_4C. The matrix alloy is melted in a graphite crucible and after melting, samples are prepared using both processes: mechanical stirring and ultrasonic process, respectively. For the MS, the mechanical stirrer is introduced in the melted metal up to the one-third position from the bottom with a stirring speed of 700 rpm. The preheated nB_4C particles are added with a pouring rate of 1 g/min (approximately) in molten metal and the stirring process is continued for 10 min, then samples are fabricated. In the case of the UST, the ultrasonic probe is introduced in molten metal to about 10 mm from the surface. The probe transmits high-intensity ultrasonic soundwaves of 15 μm in amplitude and a frequency of 20 kHz with a power of 2 kW to create the cavitation effect for 10 min into molten metal. The melted metal matrix composites are poured in a preheated mold and after solidification cast samples are prepared following the above steps.

After, solidification samples are cut and prepared for characterization and testing. The characterization is performed by SEM, BSE and EDS using field emission scanning electron microscope (FESEM) (JEOL, model: JSM7610F). The samples prepared according to ASTM standards are used for measuring mechanical properties: hardness using Brinell hardness testing machine (B 3000 H, Saroj), with a steel ball intender of 10 mm diameter and 500 kgf load for 15 seconds dwell time (ASTM E10), tensile testing samples (ASTM E8) prepared with gauge length 50 mm, the diameter of reduced section 12.5 mm and radius of fillet 10 mm. The tensile test is performed on a computerized universal testing machine (AEC1112-60T, Ashian engineers). The wear tests are performed on a pin-on-disc tribometer (DUCOM, Model TR-20LE) at the dry sliding condition and room temperature 28–32°C. The samples are prepared in pin form for a wear test of diameter 10 mm and height 30 mm machined from fabricated composite. EN31 material rotating disc of hardness 63 HRC is used against the stationary pin which is held normal to the rotating disc surface. Before starting each experiment, the surface of the pin and the rotating disc is cleaned using acetone to ensure proper contact between the pin and disc. The parameters considered for performing the wear experiments are applied loads of 10, 30 and 50 N, sliding speeds of 1.25, 2.5 and 3.7 m/s, the constant sliding

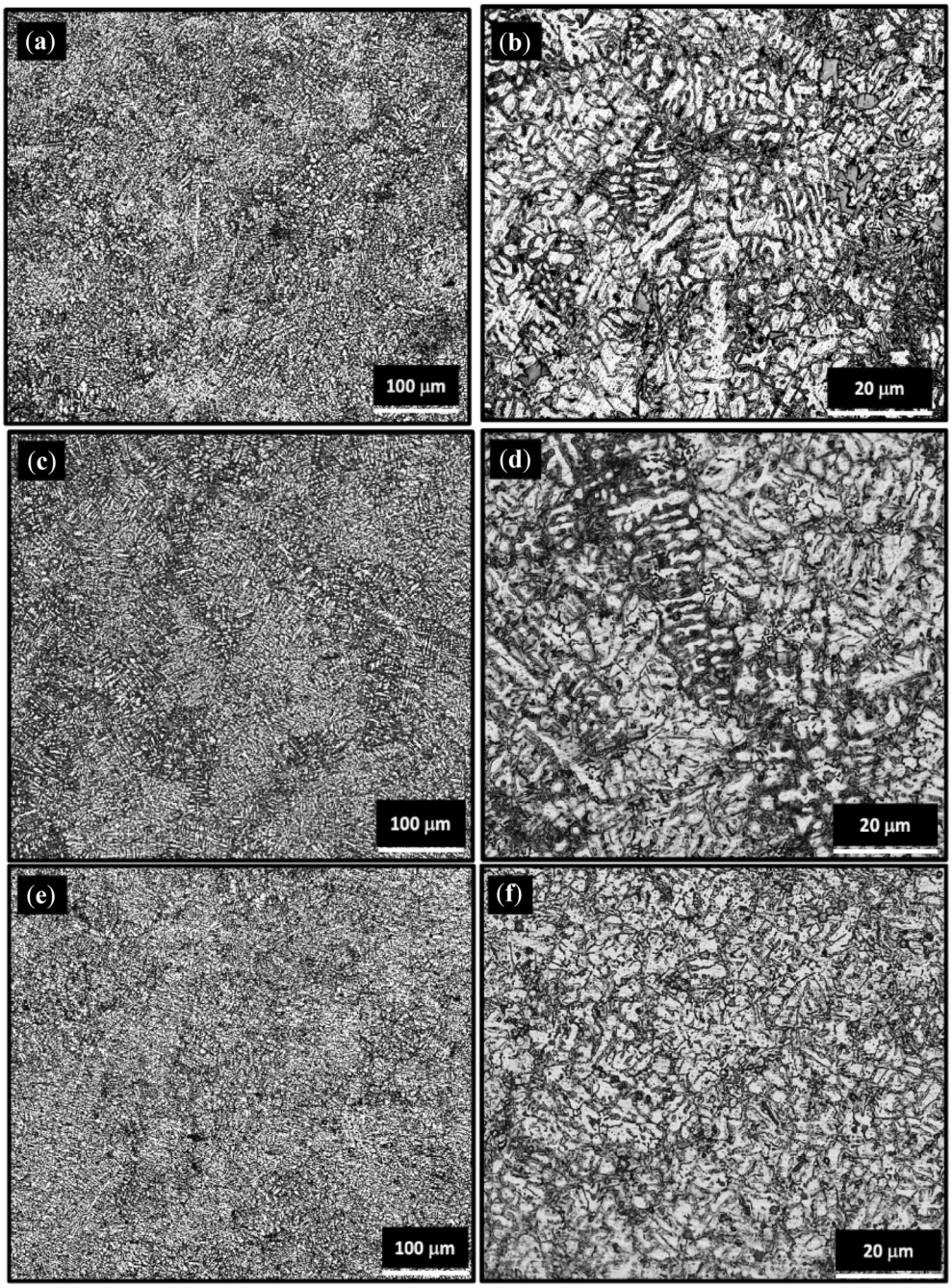

Figure 5. Optical images of Alloy A380 (a, b) without any process, (c, d) processed by MS and (e, f) processed by UST.

distance of 1500 m and constant 120 mm sliding track diameters. In order to calculate the mass loss in the pin, a weighing machine of 0.01 mg least count is used to measure the initial and final weight of the pin. The wear in the form of mass loss on the pin is calculated to subtract the final weight from the initial weight of the pin. Finally, using the results from the characterisation and testing, the effect of fabricating processes and different weight percentages of nB_4C on aluminium alloy A380 is analyzed.

3. Results and discussion

It consists of characterization of the nB_4C powder, aluminium A380 and fabricated A380/*x*-nB_4C composites using mechanical stirring (MS) and ultrasonic treatment (UST). Further, the mechanical properties of Ultimate tensile strength (UTS) and % elongation (%E), Brinell hardness (BHN) and wear (in weight loss, g) are observed of the base alloy and fabricated composites.

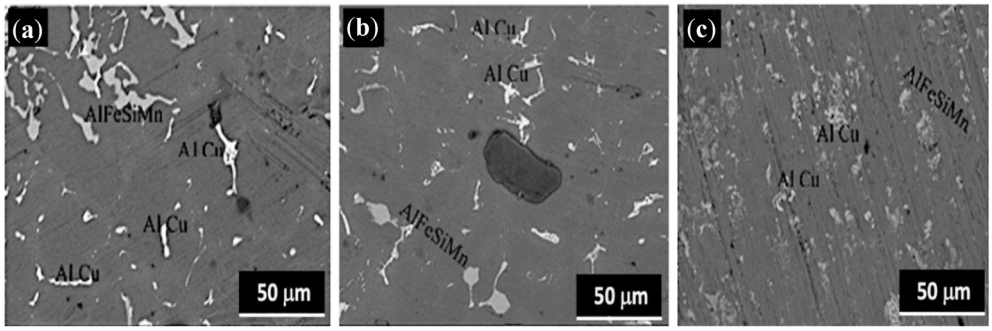

Figure 6. BSE images (a) without any process, (b) processed by MS and (c) processed by UST.

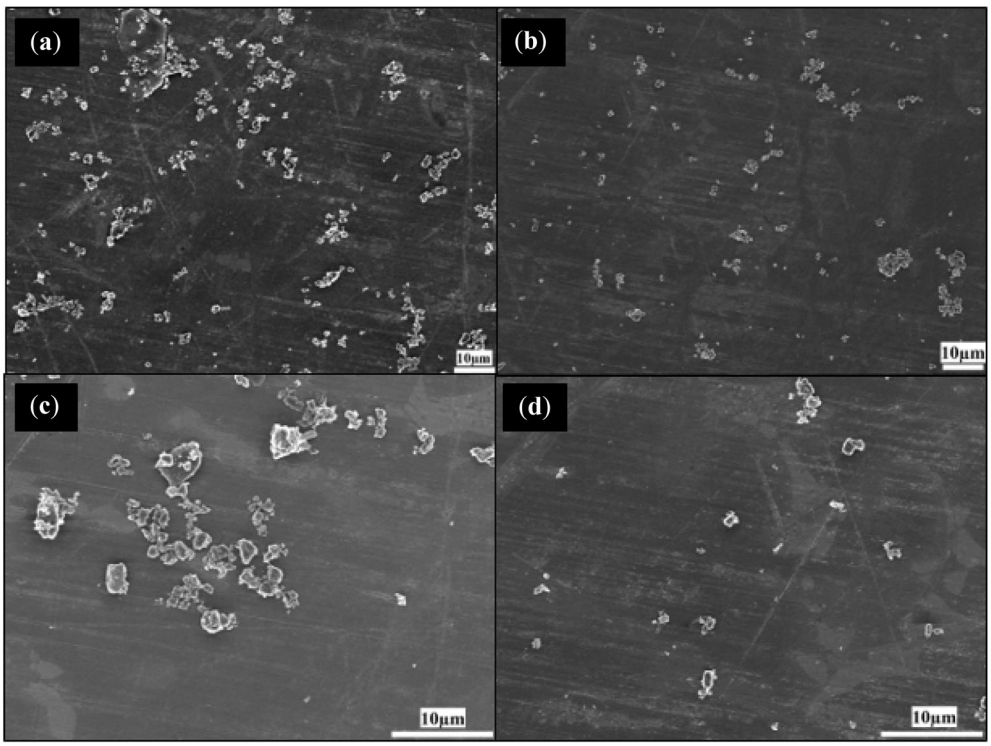

Figure 7. SEM images of selected areas (a, c) A380/1.5nB_4C (MS) and (b, d) A380/1.5nB_4C (UST).

3.1 *Characterization of A380 ingot and nB_4C powder*

The composition of aluminium A380 ingot and the nB_4C powder are shown in tables 1 and 2, respectively. The bright grey spots in figure 2(a) shows the presence of other elements with aluminium and it is confirmed from the XRD profile of ingot A380 as shown in figure 2(b). The peaks at 2θ values for Aluminium (Al) are 38.508°, 44.763°, 65.162°, 78.312° (Reference Code 98-005-3774) with miller indices (111), (002), (022), (113), respectively. Silicon (Si) shown in XRD profile with 2θ values of 28.418°, 47.293°, 56.110°, 69.115° (Reference Code-98-005-3783) and (111), (022), (113), (004) miller indices, respectively. The presence of Iron (Fe) in A380 is indicated by peaks with 2θ values of 44.484°, 64.729° (Reference Code-96-901-3475) with miller indices (011), (020) respectively. The composition of nB_4C and carbon is confirmed by the XRD profile in figure 3, in which higher peaks related to boron carbide particles and carbon peaks are low in height and less in numbers. The characteristic peaks with 2θ values of 23.448°, 34.901°, 37.694° (Reference Code-98-061-2566) and corresponding miller indices are (012), (104), (101), (021) respectively. The average particle size of nB_4C powder is less than 100 nm (figure 4) and having a hexagonal structure.

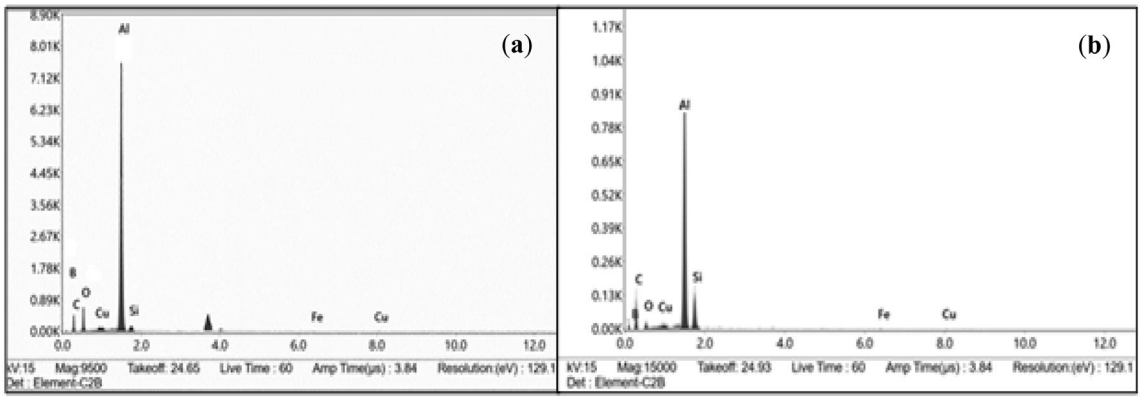

Figure 8. EDS images of (a) A380/1.5nB_4C (MS) and (b) A380/1.5nB_4C (UST).

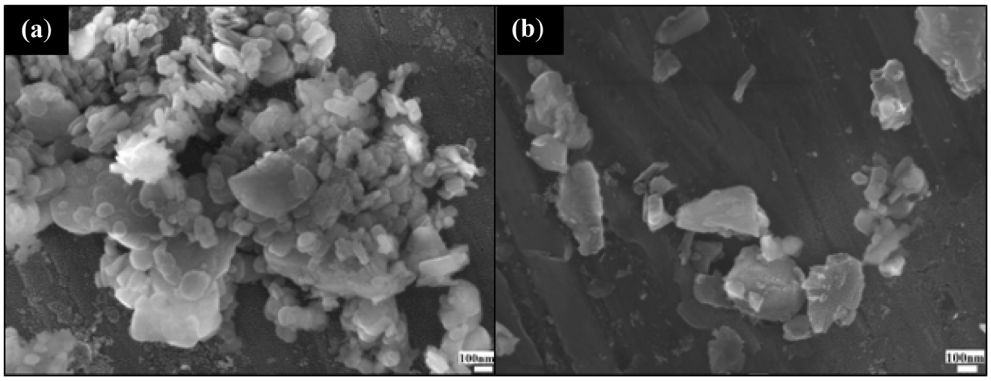

Figure 9. SEM images at higher magnification (a) A380/1.5nB_4C (MS) and (b) A380/1.5nB_4C (UST).

Table 3. Data from the mechanical properties measured.

Sl. No.	Combination	Process	UTS (MPa)	Standard Deviation (UTS)	Hardness (BHN)	Standard Deviation (Hardness)
1	A380/0nB_4C	Mechanical stirring (MS)	123.5	17.0	64.2	5.4
2	A380/0.5nB_4C		168.7	5.6	78.0	1.5
3	A380/1nB_4C		176.2	9.3	82.8	3.9
4	A380/1.5nB_4C		161.7	2.1	75.0	0
5	A380/0nB_4C	Ultrasonic treatment (UST)	130.1	19.6	69.5	4.5
6	A380/0.5nB_4C		182.7	6.6	81.2	1.4
7	A380/1nB_4C		186.5	8.5	83.5	2.5
8	A380/1.5nB_4C		178.3	4.4	79.7	0.6

3.2 *Characterization of A380 and fabricated composites*

Figure 5 represents optical micrographs of aluminium A380, first the as-cast A380 micrograph (see figure 5(a) and (b)). Comparing the sample images, the MS process helps to refine the as-cast A380 structure (figure 5(c) and (d)) however, shows less than the obtained in the casted sample using ultrasonic treatment as seen in figure 5(e) and (f). The UST has a considerable effect on the microstructure of the material due to ultrasonic cavitation as described by Eskin and Eskin [30]. In the cavitation process at the low-pressure formation of tiny bubbles occurred and these tiny bubbles

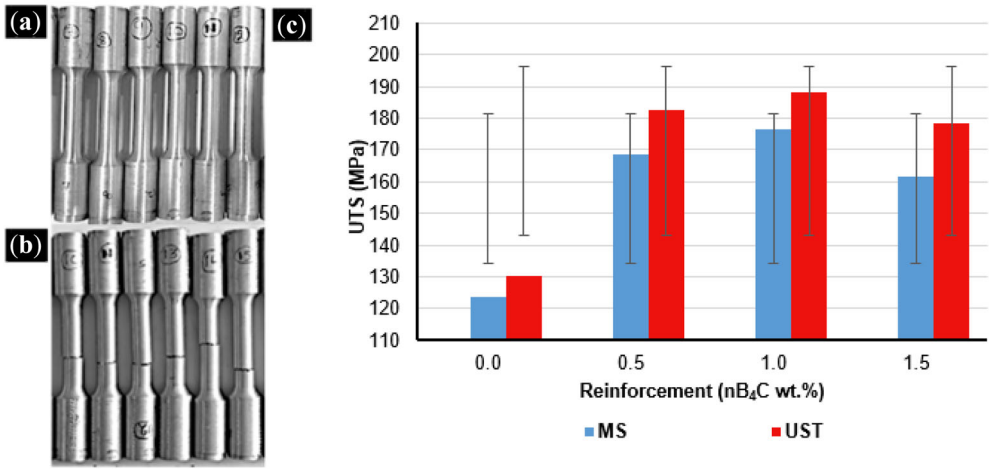

Figure 10. (a) samples of Tensile specimens before testing, (b) Tensile specimens after testing and (c) illustration of the effect of the reinforcement's percentage on the UTS.

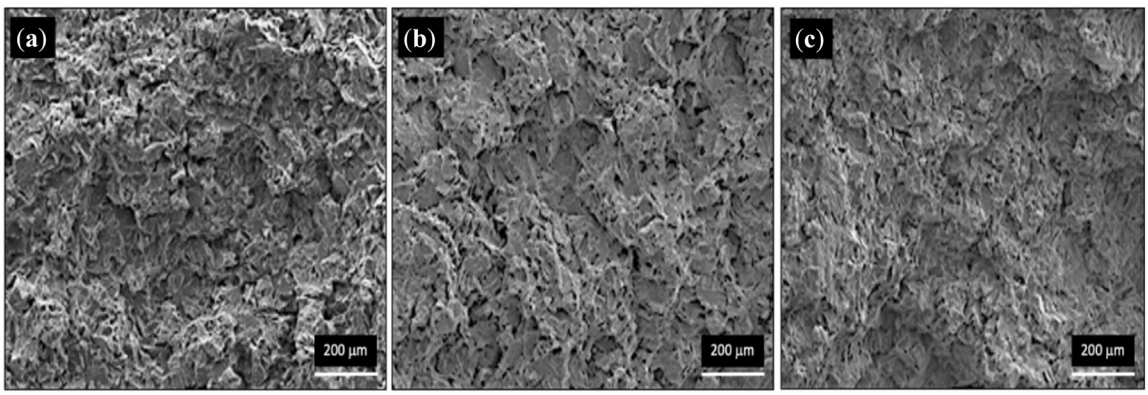

Figure 11. SEM images of fractured tensile specimens from: (a) as-Cast A380, (b) A380/1.5nB_4C (MS) and (c) A380/1.5nB_4C (UST).

collapsed with each other at high-pressure conditions produced a shock wave. The produced wave fragments the dendrites and refines the microstructure. The authors describe that the UST helps in the degassing and modification of microstructure during the solidification process. The same effect of the ultrasonic treatment is observed in the fabricated composite A380/0.5nB_4C, as shown by the phase distribution in the BSE micrograph (see figure 6(c)). Comparing images in figure 6, the ultrasonic treatment fragmented and uniformly distributes the intermetallic compounds formed during solidification (figure 6(c)), figure 6(b) shows the distribution of intermetallic compounds processed by MS, this is larger in size and less-uniformly distributed, however, having a refining effect as compared to the as-cast A380 seen in figure 6(a). The same effect of the ultrasonic treatment on intermetallic compounds is described by Zhang *et al* [31].

Figure 7 shows SEM images of the nB_4C reinforcement particles, first in the A380/1.5nB_4C composite fabricated using mechanical stirring (see figure 7(a)) and the same composite using the ultrasonic treatment (figure 7(b)). The presence of the nB_4C is confirmed for both processed samples with the EDS analysis in figure 8. In the same, it is observed the characteristic A380 peaks (Al, Si and Cu) and the Boron (B) and Carbon (C) peaks for the nB_4C in the same images.

From these images and the characterization of the different composites, it is possible to say that there is a difference in the reinforcement dispersion and distribution due to the processing method. In general, the MS-processed composites show larger agglomerations of the nB_4C as compared to the UST-processed composites. As for the nB_4C dispersion, there is also more dispersion of reinforcement materials in the UST-processed composites as compared to MS-processed as seen in figure 7(a), (b), (c) and (d). Larger magnification images of selected areas from figure 7 show the difference in the agglomerations' characteristics due to the MS (see figure 9(a)) and the UST-

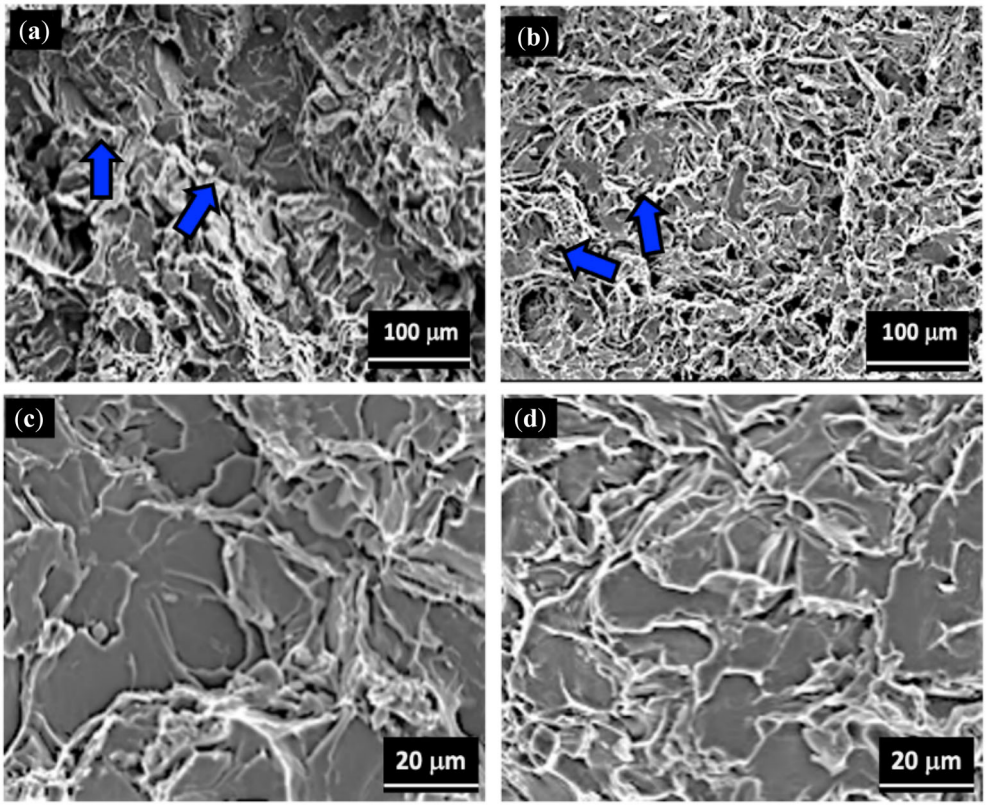

Figure 12. Higher magnification SEM images of fracture tensile specimens A380/1.5nB_4C processed by: (a) and (c) mechanical stirring and (b) and (d) by ultrasonic treatment.

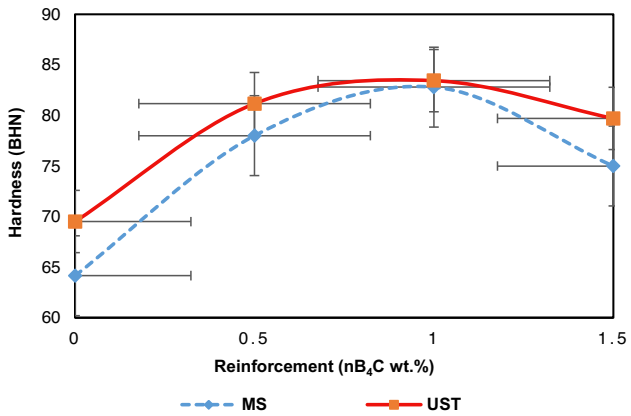

Figure 13. Effect of reinforcement on the hardness.

processed samples (see figure 9(b)), confirming that the dispersion of the nB_4C is more efficient by the UST-processing.

3.3 *Mechanical properties*

The different combinations used for fabricating A380/nB_4C composite and tensile and hardness are carried out and experimental outcomes are represented in table 3. The ultimate tensile strength and Brinell hardness for base alloy A380 without any process are 118.5 MPa and 61.7, respectively.

3.3a *Tensile Strength*: Figure 10(a) and (b) show tensile specimens before and after the tensile test respectively. Firstly, by comparing UTS of samples without any reinforcement for ultrasonic treatment and mechanical stirring, the UST process provides higher values, due to the refined grains structure achieved in ultrasonic treatment seen in figure 5(e) and (f), and previously described by Lei *et al* [32]. Table 3 shows how the refining in the microstructure is reflected in the as-cast tensile strength properties. The ultimate tensile strength (UTS) is improved from as-cast A380, to about 4% and 10% using the MS and UST treatments respectively (see figure 10(c)). Improvements occur in the fabricated composites and can vary because of the reinforcement percentage, the efficiency in the distribution and dispersion of the reinforcements. fractured tensile samples with different heights in the fractured samples showing the effect of the distribution of the reinforcements. Thereafter an increment is expected in the tensile strength of AMMC due to the presence of harder and stiffer B_4C particles in the matrix material. When the load is applied to the composites, B_4C particles provide more resistance

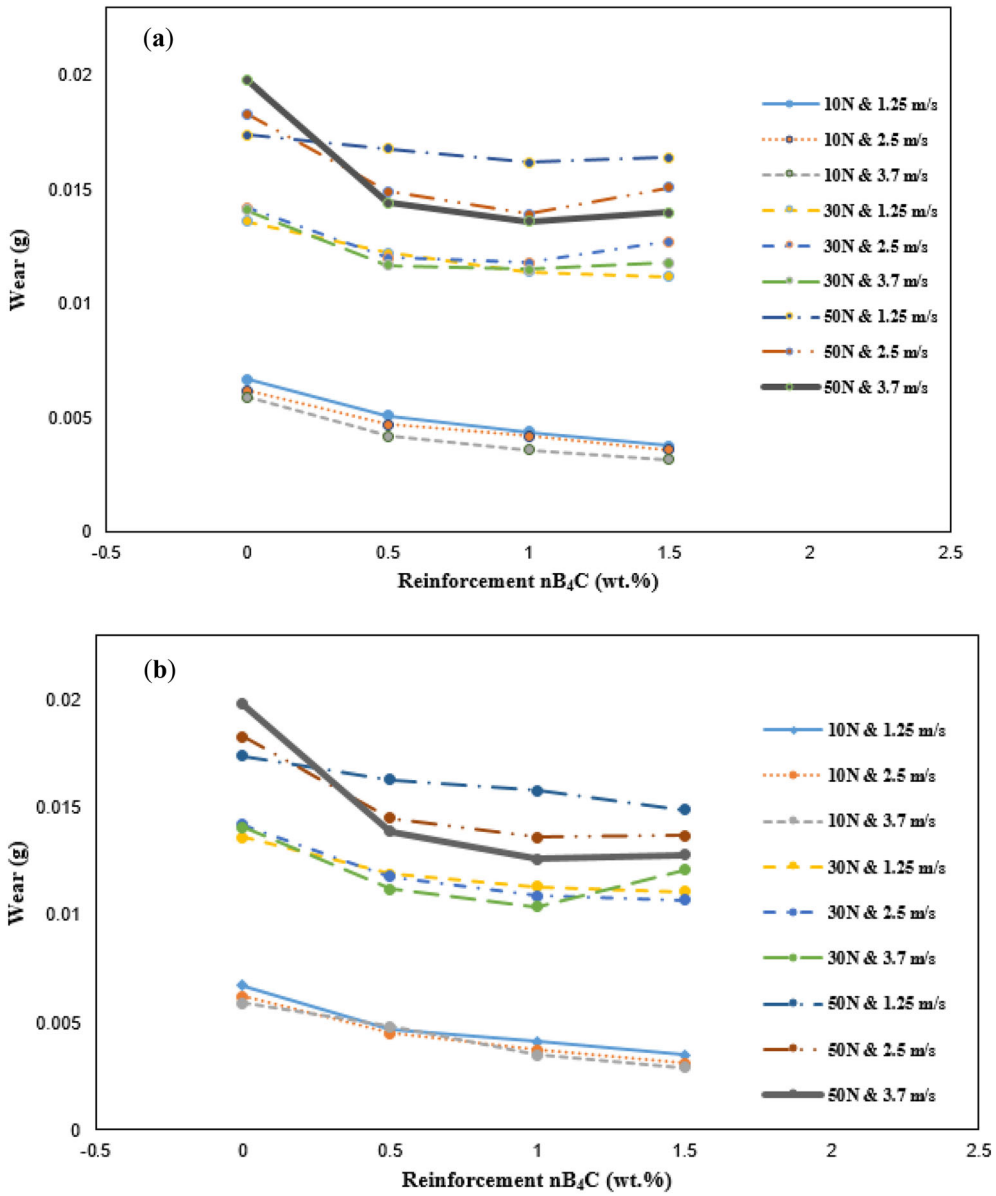

Figure 14. Wear vs reinforcement graph (a) MS, (b) UST at different applied load and sliding speed conditions.

against plastic deformation due to load transfer from matrix material to reinforced particles. With the increase in the wt.% of reinforced particle, the tensile strength of the composites increased up to a given percentage when the agglomerations drawnback the reinforcement effect as seen in figure 10(c) for the A380/1.5nB_4C. Furthermore, the tensile strength of the composite is also increased due to the thermal mismatch strengthening mechanism. In this mechanism, the residual stresses are induced in the composite due to the difference in the thermal expansion coefficient of matrix material A380 (21.8 μm/m°K) and reinforcement nB_4C (5.73 μm/m°K). These residual stresses act as a barrier to the motion of dislocations after the load is applied. Hence more load is required to move the dislocations near the induced residual stresses area, which result in higher tensile strength [16, 33]. Also, figure 10(c) shows the UTS of the A380/nB_4C (0, 0.5, 1 and 1.5 wt.%) composite fabricated by mechanical stirring and ultrasonic process. For both the processes, the UTS of the composite increased with wt.% 0.5 and 1.0 and then decrease at wt.% 1.5 of nB_4C. The composite contains nB_4C in wt. 1% provides the highest UTS with the use of ultrasonic. Equal quantity of B_4C particles, UTS for ultrasonic treatment is higher as compared with mechanical stirring.

Figure 11 indicates the brittle fracture cleared from the facets in large numbers in tensile testing. At 1.5 wt.% of reinforced particles, the UTS of composite prepared using

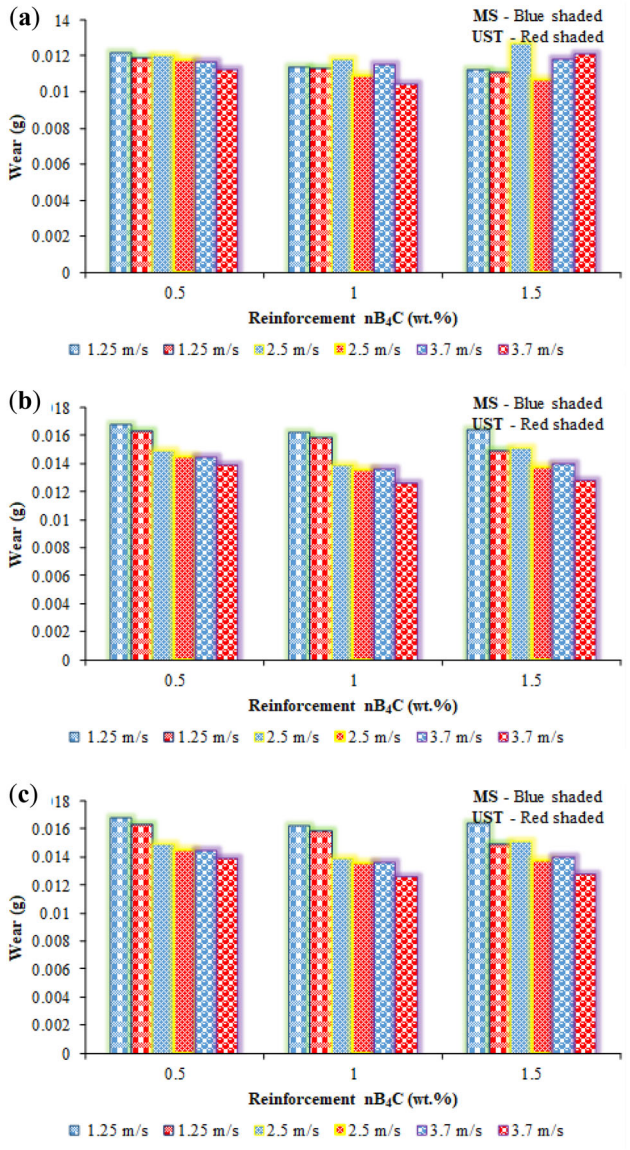

Figure 15. Wear-reinforcement graphs at different load and speed conditions (a) Load 10 N, (b) Load 30 N and (c) Load 50 N.

both the processes decreases due to the porosity present in the composite as shown in figure 11 and the brittle agglomerations seen in the same images. Figure 12 shows a larger view of fractured samples of A380/1.5nB_4C processed by MS and UST. Arrows in these figures help in the visual comparison between the prominent debonding behaviour of the MS composites and the more uniform and smaller debonding occurring in the UST-processed samples. Examples of the agglomerated reinforcement particles, the sliding and ductility of the A380 matrix are shown in the larger magnification images taken from selected areas in figure 12(a) and (b). Figure 12(c) exhibits less ductility and larger de-bonded areas, accompanied by large agglomerations of nB_4C reinforcements as compared to the same features in figure 12(d). Figure 12(d) shows smaller agglomerations and more ductile areas in comparison indicating a more homogeneous distribution and dispersion of the reinforcements. However, as compared to the UST efficiency, the MS-processed composites exhibit lower efficiency attributed to the intense stress concentrations that occurred near particles agglomeration after load applied, causing the premature fractures and large debonding areas observed in figure 12(a) for the MS-processed composites.

In general, the elongation percentage is measured to be less than the 0.95%E (% elongation) for the A380 Ingot. The decrease ranges from 5 to 11% for the MS-processed composites. For the UST-processes composites, the reduction is from 10 to 21%, however, an improvement is observed and measured in the A380/1nB_4C composites at 1.05%E, representing an increase of about 10%. As a result, the UTS values observed from the fabricated A380/nB_4C composites is much higher than that of base alloy A380 values.

3.3b *Hardness*: The hardness of the different A380/nB_4C (0, 0.5, 1, 1.5%) composites fabricated by MS and UST are indicated in figure 13. The hardness value of the composite developed via both processes increases with wt.% 0, 0.5 and 1.0 and then decreases at wt.% 1.5 of nB_4C. With the addition of the nB_4C particles in base metal, the hardness of composite increased due to resistance offered by hard particles of nB_4C. An increment of 4% and 13% is measured after the initial A380 alloy is processed by the MS and UST respectively. During the test, while the steel indenter moves downward, nB_4C particles present in the sample act as a barrier against indentations and show a higher value of hardness. Figure 13 shows that the hardness values from the UST cast samples are higher than MS cast samples for all the wt.% additions of nB_4C, however, the highest values are shown in the A380/1nB_4C. Based on the as-cast hardness the composites´ hardness increase up to 33% and 35% in the samples processed by the MS and UST respectively. Then, the hardness of the composites prepared using 1.5 wt.% of nB_4C particles shows decrement for both the processes due to the presence of micro-porosities and the agglomerated nB_4C particles.

3.4 *Wear behaviour*

The wear of the base alloy and fabricated composite is calculated in weight loss and measured in grams. The experiments are performed on pin-on-disk apparatus to evaluate the effect of load, sliding speed and reinforcement on wear at dry sliding conditions. The effect of different loads, sliding speeds and different weight percentages of reinforced particles for MS and UST processes are indicated in figure 14. An increase in the quantity of reinforcement (0.5–1.5 wt.%), the wear for

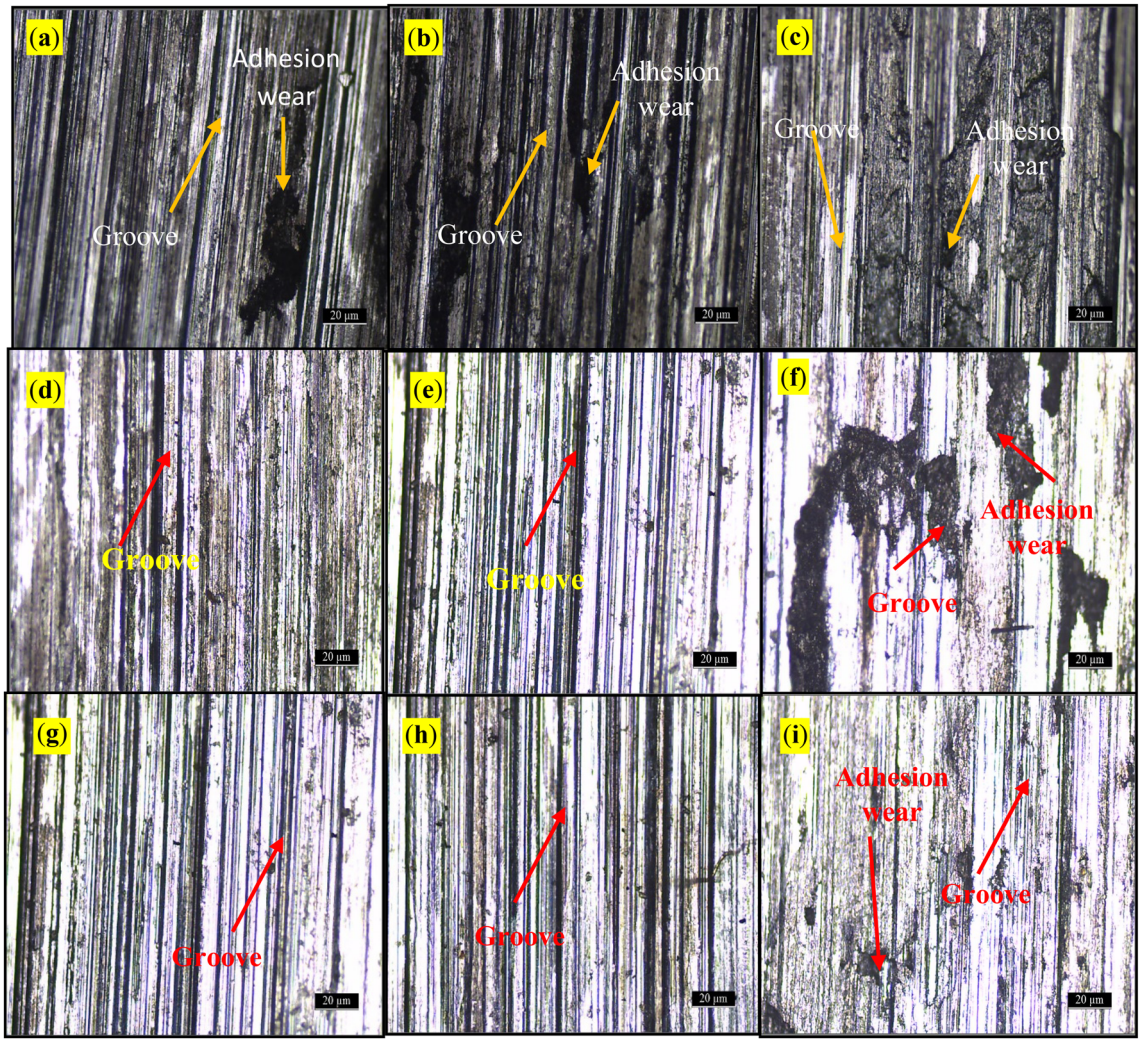

Figure 16. Optical images at various speed (1.25 m/s, 2.5 m/s, 3.7 m/s) and load (10 N, 30 N, 50 N) (a, b, c). Base alloy without any process (d, e, f) UST (1.5 wt.% nB_4C), (g, h, i) MS (1.5 wt.% nB_4C).

the composite samples fabricated using MS and UST processes is reduced with an increase in sliding speed (1.25–3.7 m/s) and wear increased with an increase in applied load (10–50 N). Furthermore, with the increase in applied load and sliding speed, the wear loss for alloy A380 is more in comparison to fabricated composites because the non-reinforced aluminium alloy is softer than the reinforced composite. In the case of composite, at 10 N load, 1.5 wt.% nB_4C and sliding speed of 3.7 m/s attained minimum wear in case of UST process as shown in figure 14(b). The highest wear is occurred at a sliding speed of 1.25 m/s, applied load of 50 N and 0.5 wt.% nB_4C in MS process as indicated in figure 14(a). At sliding speeds of 3.7 m/s and applied load 30 N and 50 N, the wear loss is less as compared to sliding speeds of 1.25 m/s and 2.5 m/s due to the formation of the boron oxide layer. With an increase in load, the base alloy undergoes plastic deformation, exhibited heavy weight loss at every applied load condition. Further, at a higher applied load, the weight loss is increased with an increase in sliding speed due to a rise in temperature at the contact point. The developed composite exhibited less wear due to resistance offered by the hard nB_4C particles. During the wear test, in the presence of B_4C particles, the composites formed a mechanically mixed layer (MML), the formed layer replaced the actual layer of composite to offered resistance against the rotating disk. MML region showed higher hardness as compared to the non-MML area [34–36]. The wear comparison for MS and UST processes at different wt.% of reinforcement, loads and speeds is shown in figure 15. At all conditions of applied load (10–50 N), sliding speed (1.25–3.7 m/s) and reinforcement (0.5–1.5 wt.%), UST processed fabricated composites show better wear resistance as compared to MS as indicated in figure 15(a), (b), (c).

3.5 *Analysis of wear surfaces*

The optical microscopic images of wear surfaces for base alloy and fabricated composites are shown in figure 15. It is cleared from Figure 16(a), (b), (c) base alloy showed abrasive and adhesion wear with increased in applied load and sliding velocity. At applied load 10 N and sliding speed 1.25 m/s, the base alloy exhibited abrasive wear and with an increase in load (30 N, 50 N) and speed (2.5 m/s, 3.7 m/s) adhesion wear is more as compared to abrasive wear. In the case of composite, the abrasive wear is dominating as compared to adhesion wear fabricated using MS and UST processes. In composite, when the applied load (10–30 N) and speed (2.5 m/s, 3.7 m/s), the grooves are formed on the surface, which proved abrasive wear for both the fabricated processes (figure 16(d), (e), (g), (h)). When applied load is 50 N and speed 3.7 m/s the composite fabricated using MS showed more adhesion wear as compared to UST processed composite as indicated in figure 15(f), (i).

4. Conclusions and future scope

Aluminium A380/x-nB_4C metal matrix composites are fabricated via mechanical stirring and ultrasonic treatment processes and the microstructure, wear and mechanical properties of the composites are investigated. The following conclusions are presented from this analysis.

- The microstructure of samples is found to be more refined in the UST process as compared to MS. The reinforced particles are efficiently and uniformly distributed in UST processed.
- The highest values of UTS are achieved at A380/1nB_4C particles via ultrasonic treatment. The lowest UTS is found in the A380/1.5nB_4C composites fabricated by mechanical stirring; this reduction is attributed to the large agglomerations of reinforcement particles.
- The hardness values are higher for both processes (MS and UST) as compared to the base metal.
- The wear of fabricated composites and the base alloy is increased with applied load and show a reverse effect with an increase in the quantity of reinforcement and sliding speed.
- Ultrasonic treatment is an efficient process as compared to mechanical stirring to achieve enhanced mechanical properties.

The present research work is done for a specified time (10 min) using an ultrasonic treatment process. The future scope of this research work will be to perform the experiments at different timings with ultrasonic treatment (UST) and weight percentages in the route to optimize the performance of these composites. Finally, to determine constants for tailoring the properties for specific industrial applications.

Acknowledgements

The authors would like to thank the Department of Mechanical Engineering, Sant Longowal Institute of Engineering and Technology (SLIET) Longowal, Punjab, India for providing the testing facilities. The authors would also like to thank Mr Ravi Kumar for providing the machining facilities at Siddh Auto Components Faridabad, Haryana, India.

References

[1] Singh J and Chauhan A 2019 A review of microstructure, mechanical properties and wear behavior of hybrid aluminium matrix composites fabricated via stir casting route. *Sādhanā* 44: 1–18

[2] Liu S, Wang Y, Muthuramalingam T and Anbuchezhiyan G 2019 Effect of B_4C and MOS_2 reinforcement on microstructure and wear properties of aluminium hybrid composite for automotive applications. *Compos. Part B Eng.* 176: 107329

[3] Qiu X, Qi L, Tang J R, Cui X Y, Du H, Wang J Q and Xiong T Y 2020 Influence of particulate morphology on microstructure and tribological properties of cold sprayed A380/Al_2O_3 composite coatings. *J. Mater. Sci. Technol.* 44: 9–18

[4] Gencalp S and Saklakoglu N 2010 Semisolid microstructure evolution during cooling slope casting under vibration of A380 aluminum alloy. *Mater. Manuf. Process.* 25: 943–947

[5] Suresh S, Gowd G H and Kumar M D 2019 Experimental investigation on mechanical properties of Al 7075/Al_2O_3/Mg NMMC's by stir casting method. *Sādhanā* 44: 51

[6] García-Rodríguez S, Alba-Baena N, Rudolph N M, Wellekoetter J, Li X C and Osswald T A 2012 Dimensional analysis and scaling in mechanical mixing for fabrication of metal matrix nanocomposites. *J. Manuf. Process.* 14: 388–392

[7] Bhushan R K and Kumar S 2011 Influence of SiC particles distribution and their weight percentage on 7075 Al alloy. *J. Mater. Eng. Perform.* 20: 317–323

[8] Kumar D and Singh P K 2019 Microstructural and mechanical characterization of Al-4032 based metal matrix composites. *Mater. Today Proc.* 18: 2563–2572

[9] Auradi V and Kori S A 2014 Preparation and evaluation of mechanical properties of 6061Al-B_4Cp composites produced via two-stage melt stirring. *Mater. Manuf. Process.* 29: 194–200

[10] Yu L I, Li Q L, Dong L I, Wei L I U and Shu G G 2016 Fabrication and characterization of stir casting AA6061—31% B_4C composite. *Trans. Nonferrous Met. Soc. China* 26: 2304–2312

[11] Park B, Lee D, Jo I, Lee S B, Lee S K and Cho S 2020 Automated quantification of reinforcement dispersion in B_4C/Al metal matrix composites. *Compos. Part B Eng.* 181: 107584

[12] Alba-Baena N, Pabel T, Villa-Sierra N and Eskin D G 2013 Effect of ultrasonic melt treatment on degassing and structure of aluminium alloys. *Mater. Sci. Forum* 765: 271–275 (**Trans Tech Publications Ltd.**)

[13] Singh S, Gupta A, Sharma V S and Harichadaran R 2019 Production and high temperature wear characterization of AA 7075/Al_2O_3/Graphite hybrid nanocomposites by enhanced stir and ultrasound assisted casting method. *Mater. Res. Express* 6: 125072

[14] Miranda A, Alba-Baena N, McKay B J, Eskin D G, Ko S H and Shin J S 2013 Study of mechanical properties of an LM24 composite alloy reinforced with Cu-CNT nanofillers, processed using ultrasonic cavitation. *Mater. Sci. Forum* 765: 245–249 (**Trans Tech Publications Ltd.**)

[15] Gudipudi S, Nagamuthu S, Subbian K S and Chilakalapalli S P R 2020 Enhanced mechanical properties of AA6061-B_4C composites developed by a novel ultra-sonic assisted stir casting. *Eng. Sci. Technol. Int. J.* 23: 1233–1243

[16] Harichandran R and Selvakumar N 2016 Effect of nano/micro B_4C particles on the mechanical properties of aluminium metal matrix composites fabricated by ultrasonic cavitation-assisted solidification process. *Arch. Civ. Mech. Eng.* 16: 147–158

[17] Baradeswaran A E P A and Perumal A E 2013 Influence of B_4C on the tribological and mechanical properties of Al 7075–B_4C composites. *Compos. Part B Eng.* 54: 146–152

[18] Sun C, Song M, Wang Z and He Y 2011 Effect of particle size on the microstructures and mechanical properties of SiC-reinforced pure aluminum composites. *J. Mater. Eng. Perform.* 20: 1606–1612

[19] Choi H, Alba-Baena N, Nimityongskul S, Jones M, Wood T, Sahoo M, Lakes R, Kou S and Li X 2011 Characterization of hot extruded Mg/SiC nanocomposites fabricated by casting. *J. Mater. Sci.* 46: 2991–2997

[20] Yang Y, Lan J and Li X 2004 Study on bulk aluminum matrix nano-composite fabricated by ultrasonic dispersion of nano-sized SiC particles in molten aluminum alloy. *Mater. Sci. Eng. A* 380: 378–383

[21] Yang Y and Li X 2007 Ultrasonic cavitation based nanomanufacturing of bulk aluminum matrix nanocomposites. *J. Manuf. Sci. Eng.* 129: 497–501

[22] Khakbiz M and Akhlaghi F 2009 Synthesis and structural characterization of Al–B_4C nanocomposite powders by mechanical alloying. *J. Alloys Compd.* 479: 334–341

[23] Nie C Z, Gu J J, Liu J L and Zhang D 2007 Production of boron carbide reinforced 2024 aluminium matrix composites by mechanical alloying. *Mater. Trans.* 48: 990–995

[24] Alizadeh A and Taheri-Nassaj E 2012 Mechanical properties and wear behavior of Al–2 wt.% Cu alloy composites reinforced by B_4C nanoparticles and fabricated by mechanical milling and hot extrusion. *Mater. Charact.* 67: 119–128

[25] Liu X, Jia S and Nastac L 2014 Ultrasonic cavitation-assisted molten metal processing of cast A356-nanocomposites. *Int. J. Metalcast.* 8: 51–58

[26] Arulraj M and Palani P K 2018 Parametric optimization for improving impact strength of squeeze cast of hybrid metal matrix (LM24–SiC p–coconut shell ash) composite. *J. Braz. Soc. Mech. Sci. Eng.* 40: 2

[27] Bouazara M, Bouaicha A and Ragab K A 2015 Fatigue characteristics and quality index of A357 type semi-solid aluminum castings used for automotive application. *J. Mater. Eng. Perform.* 24: 3084–3092

[28] Kareem A, Qudeiri J A, Abdudeen A, Ahammed T and Ziout A 2021 A Review on AA 6061 metal matrix composites produced by stir casting. *Materials* 14: 175

[29] Ezatpour H R, Sajjadi S A, Sabzevar M H and Huang Y 2014 Investigation of microstructure and mechanical properties of Al6061-nanocomposite fabricated by stir casting. *Mater. Des.* 55: 921–928

[30] Eskin G I and Eskin D G 2014 Ultrasonic treatment of light alloy melts. CRC Press. p. 129–168. https://doi.org/10.1201/b17270

[31] Zhang Y, Jie J, Gao Y, Lu Y and Li T 2013 Effects of ultrasonic treatment on the formation of iron-containing intermetallic compounds in Al-12% Si-2% Fe alloys. *Intermetallics* 42: 120–125

[32] Lei J, Yu J, Chen J, Li C, Luo H and Li Z 2018 Effect of trace Sr and Sc contents and ultrasonic vibration on the microstructure and mechanical properties of the A380 alloy. *Adv. Mech. Eng.* 10: 1–9

[33] Zhang Z and Chen D L 2008 Contribution of Orowan strengthening effect in particulate-reinforced metal matrix nanocomposites. *Mater. Sci. Eng. A* 483: 148–152

[34] Rosenberger M R, Schvezov C E and Forlerer E 2005 Wear of different aluminum matrix composites under conditions that generate a mechanically mixed layer. *Wear* 259: 590–601

[35] Uvaraja V C, Natarajan N and Sivakumar K 2015 Tribological behavior of heat treated Al 7075 aluminium metal matrix composites. *Indian J. Eng. Mater. Sci.* 22: 51–61

[36] Demirel M and Muratoglu M 2011 Influence of load and temperature on the dry sliding wear behavior of aluminium-Ni 3 Al composites. *Indian J. Eng. Mater. Sci.* 18: 268–282